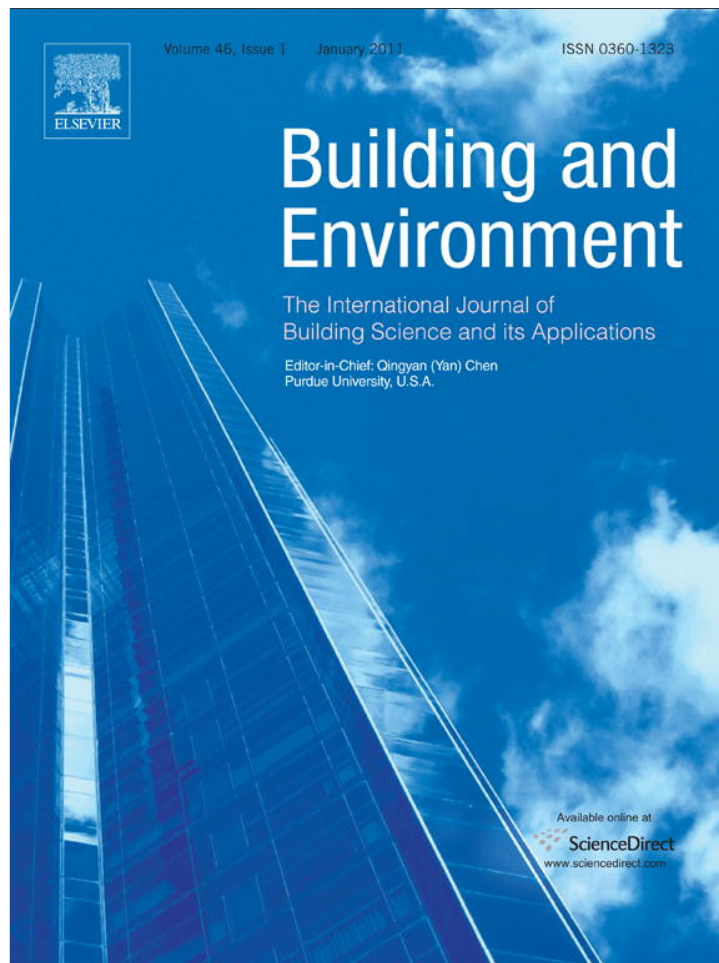


Provided for non-commercial research and education use.
Not for reproduction, distribution or commercial use.



(This is a sample cover image for this issue. The actual cover is not yet available at this time.)

This article appeared in a journal published by Elsevier. The attached copy is furnished to the author for internal non-commercial research and education use, including for instruction at the authors institution and sharing with colleagues.

Other uses, including reproduction and distribution, or selling or licensing copies, or posting to personal, institutional or third party websites are prohibited.

In most cases authors are permitted to post their version of the article (e.g. in Word or Tex form) to their personal website or institutional repository. Authors requiring further information regarding Elsevier's archiving and manuscript policies are encouraged to visit:

<http://www.elsevier.com/copyright>



Contents lists available at SciVerse ScienceDirect

Building and Environment

journal homepage: www.elsevier.com/locate/buildenv

Experimental and computational investigation of indoor air quality inside several community kitchens in a large campus

Shubhajyoti Saha, Abhijit Guha*, Subhransu Roy

Mechanical Engineering Department, Indian Institute of Technology, Kharagpur, Pin 721302, India

ARTICLE INFO

Article history:

Received 1 June 2011

Received in revised form

12 September 2011

Accepted 19 October 2011

Keywords:

Indoor air quality

Computational fluid dynamics

3-dimensional CFD

Temperature

Fluid flow field

Obnoxious gases

ABSTRACT

The present work deals with the experimental and computational investigation of the air quality in selected kitchens in the campus of a large institute in India. Four kitchens have been carefully selected after a detailed initial survey of the cooking arrangement and exhaust systems in all of the kitchens in the campus. For the experimental part, the concentrations of CO₂ and CO and temperature are recorded with the help of an indoor air quality measurement device named *IAQ Calc7545*. In each of the four kitchens, a 1.8 m × 1.5 m vertical area was selected, which is perpendicular to the vertical side of a burner that faces the cooks, and measurements were carried out at 72 suitable grid points within this area. For the computational part, the three-dimensional fluid flow field in the kitchen of site 1 is numerically simulated by Fluent. The volume fractions of CO₂ and CO at the outlet of the burners are estimated from a separate FORTRAN code for equilibrium chemical analysis and are used as a boundary condition for the Fluent simulation. The mixture model for the multiphase flow in Fluent is used for finding the distribution of the species within the flow domain. Given the complexity of the geometry and flow field considered here, the results of CFD modelling agree well with the experiments, validating the choice of boundary conditions, grid generation and other subtleties involved. The measured and computed values are compared with the corresponding ASHRAE standard.

© 2011 Elsevier Ltd. All rights reserved.

1. Introduction

Indoor air quality (IAQ) has been receiving more and more attention and increasing interest has been directed towards controlling of indoor obnoxious gases such as CO₂, CO etc. In a hostel's kitchen, working conditions are especially demanding. The air quality is affected by high emission rate of contaminants released from the cooking processes. Ventilation plays an important role in providing comfortable and productive working conditions and in securing contaminant removal. There are three main factors affecting thermal comfort, these being: air temperature, air velocity and air humidity.

In the present work, a detailed analysis is performed to study the distribution of obnoxious gases and temperature. One difficulty when attempting to predict the detailed indoor air flow is that there are many factors which influence or govern the flow. It is affected by the details of the air distribution design, building construction, outdoor environment, and the presence and activities of the human beings occupying the space, among many other

factors. When designing and analyzing heating, ventilation and air-conditioning (HVAC) systems, engineers and scientists generally have at their disposal three tools to study the indoor air flow patterns: analytical model, full scale or small scale model measurements and computational fluid dynamics (CFD). Analytical models are usually restricted by the need for simplifying assumptions and simplistic configurations. Full scale measurements can provide the most reliable data, but are most expensive and difficult (or mostly impossible) to perform. Extrapolation from small scale model data to a real size room or building is limited by scaling difficulties. CFD seems to be a general and accessible method, but this too faces several challenges. For the application of CFD to indoor air flow, the challenges include modelling the physics of the flow including turbulence, specifying realistic boundary conditions, representing the complex geometry of the room and developing accurate and efficient numerical algorithms.

The published studies demonstrate quite clearly the health risk of the cooking. Thiebaud et al. [1] indicates that the fumes generated by frying pork and beef are mutagenic. Hence the chefs are exposed to relatively high levels obnoxious gases such as CO₂, CO, air bone mutagens and carcinogens. Vainiotalo [2] carried out measurements at eight work places. The survey confirmed that cooking fumes contain hazardous components. It also indicated

* Corresponding author. Tel.: +91 3222 281768; fax: +91 3222 282278.
E-mail address: a.guha@mech.iitkgp.ernet.in (A. Guha).

that the kitchen worker may be exposed to relatively high concentrations of pollutants. The quality of indoor air is also affected by the formation, transport, and deposition [3,4] of particulate material, which have not been included in the present work.

Although cigarette smoking is considered to be the most important cause of lung cancer [5], smoking behaviour cannot fully explain the epidemiological characteristic of lung cancer among Asian women who rarely smoke but contract lung cancer relatively often. A study by Ng [5] found that over 97% of the women in Singapore do not smoke. Thus the presumable source of indoor air pollution for housewives is passive smoking and cooking. The aforementioned study indicated that greater relative odds of respiratory symptoms were associated with increasing weekly frequency of gas cooking.

The above studies establish the importance of a well-designed ventilation system in kitchens. The efficacy of the exhaust system should be especially emphasized. It can be shown that the capture efficiency of the hood equals the ratio of the capture flow rate to the total plume flow rate at the front of canopy height [6]. The total system must be designed such that the impurities are effectively removed and do not spread throughout the kitchen. The totalistic approach of ventilation design should be used to fulfil all needs of indoor air conditions. This means that the ventilation system is designed based on target values of indoor air quality (IAQ), and the actual total heat loads and emission characteristics of the kitchen appliances.

Modelling plays a key role in indoor environmental design. Computational fluid dynamics (CFD) is used for simulating air flow phenomena. CFD methods are based on the solution of the discretized form of the Navier–Stokes equations on a grid of points combined with turbulence modelling. A computational investigation [7] in a simple geometry shows the effects of main physical factors like inlet, exhaust location, air flow rate on the distribution of contaminant concentration in a workroom. The amount of ventilation in an indoor environment under various inlet and outlet arrangements has also been investigated [8] using both numerical analysis and experimental validation. Although CFD can result in more accurate predictions (as compared to analytical, semi-empirical or small scale studies) when modelling indoor spaces or localized phenomena such as drafts and acute pollutant exposures, i.e. in situations where the well-mixed assumption does not hold, special care has to be taken in defining the computational grid, in setting boundary conditions and in assigning the physical properties of the models [9]. The CFD approach is also limited by its requirements on computational costs.

The prediction from a CFD simulation regarding the accumulation of air contaminants shows how the accumulation is related to the location of gas fire in a conventional kitchen [10]. CFD can also be used for parametric modelling of domestic kitchen hood to permit the rapid modification of fundamental parameters, such as the number of blades and the twist angle of the fan [11]. This is an important point which concerns architects, designers and in some cases healthcare professionals [12]. CFD analysis predicts velocity, temperature and concentration values throughout the solution domain, and an analysis of these parameters makes it possible to infer modifications to the fluid flow patterns or boundary conditions (exhaust fans, vents). The flexibility of this methodology provides insights into engineering and architectural design alternatives for improving the indoor air environment in the kitchen.

The objective of the present work is to study, experimentally and computationally, the indoor air quality of several kitchens in the campus of a large institute in India. Four kitchens (referred to here as site 1, site 2 etc.) have been carefully selected after a detailed initial survey of all large kitchens in the campus. Sites 1, 2,

3 and 4 serve 3/4 meals/snacks for approximately 320, 300, 500 and 600 people at each meal respectively per day. The measured and computed values are to be compared with each other and with the corresponding ASHRAE standard [13].

2. Experimental method and results

The main objective of this work is to carry out air quality surveys in different hostel's and canteen's kitchens. The readings are taken without disturbing the normal working routine of the kitchen so that the measured values represent the actual working conditions. At each location, experimental measurements took about two hours per data set.

2.1. Site selection

In this experimental work, four kitchens are selected based on their type, namely: 1. a large kitchen with exhaust fans, 2. a kitchen with general or dilution ventilation system, 3. a small hot and humid kitchen, 4. a modern kitchen with local exhaust ventilation (LEV) system.

Ventilation engineers categorize systems as being either general (dilution) or local exhaust ventilation systems (LEV). The main basic form of ventilation is general or dilution ventilation [14], consisting simply of an exhaust fan pulling air out of the work place and exhausting it to the outdoor. A general ventilation system may include a replacement air system, replacement air distribution ducting, and in more rare situations, air-cleaning equipment on the exhaust stream. Local exhaust ventilation (LEV) implies an attempt to remove the contaminant at or near the point of release, thus minimizing the opportunity for the contaminant to pervade the work place. The nominal LEV system includes an exhaust hood, ducting, a fan and an exhaust outlet [14]. Some overall features about these four sites can be appreciated from Fig. 1.

2.1.1. Site 1

Site 1 is a large kitchen. There are three large windows, three doors and no hood in the kitchen. There are three exhaust fans in the kitchen. The average flow rate of each fan is 587 L/s. This average flow rate is established in the present work by measuring, with the help of a velocity anemometer, the velocity at several points over a cross-section near the fan. LPG fuel is supplied through a common pipe connected to all of the burners. The burners are in good condition giving low values of the measured CO concentration close to the burners, they also have design features that effectively spread the CO₂ produced. The experiments are performed at 3 pm onwards at site 1, because, according to the schedule, there is a large cooking activity for a sustained period. At the time of the experiment, water is boiled on two burners & frying is done on another.

2.1.2. Site 2

Site 2 is a very busy kitchen. There are four doors and three windows in the kitchen. A general or dilution ventilation system (with one hood and two exhaust fans) is used. LPG is used as the fuel. There are four burners, three of which are placed under a natural hood. The burners are not as effective as in site 1. So a large amount of CO is produced and a large concentration of CO₂ is measured near the burners. The experiment is performed at 2 pm onwards in site 2. Frying is done on the burner (at whose mid-plane the measurements are taken) at the time of the experiment.

2.1.3. Site 3

The selected kitchen has humid and hot ambience. It is a very busy and packed kitchen. It has three windows. Eight LPG cylinders,



Fig. 1. Picture of the four selected sites showing some overall features and internal arrangements.

each containing 14.2 kg of the cooking gas, are required for the purpose of cooking in the kitchen in a week. The environment is very hazardous around 8 am, when all the four burners are used simultaneously. The measurements reported in this study are therefore performed between 8 and 9 am. There are three windows (exposed to the open atmosphere) and two doors (which open into the dining hall) playing the important role for ventilation. There is no external hood over the burners. Pollutants are expelled by two exhaust fans from the kitchen, located at the top of one wall of the room.

2.1.4. Site 4

It is the most modern out of the four selected kitchens. It has a local exhaust ventilation (LEV) system for each burner, which is very effective to expel different obnoxious gases and hot air which are formed due to cooking processes. So the measured pollutant concentration is found to be very near to the acceptable range at the breathing zone plane though the measured temperature is well above the ASHRAE standard. It is a moderate size kitchen. There are four doors in the kitchen, which provide some ventilation, but there is no window at all. There are six burners, three of which are working at the time of the experiment. All burners are LPG based. Ten LPG cylinders are consumed in three days in the discussed kitchen. Three to four persons are engaged in the kitchen for cooking purpose. The working load of the kitchen is not very high.

The experiment is done at 9.00 am onwards. At the time of the experiment, potatoes and fishes are fried. The flow rate through the burner is set at its maximum. There are three exhaust fans in the kitchen. The average flow rate through an exhaust fan is measured as 2550 L/s: as compared to the other kitchens, the fans are larger in size and are in relatively better condition. The outlets of the ventilator and exhaust fans are accessible in this site and hence an additional set of measured data for the pollutant concentration is recorded in this case. The measured concentrations of CO₂ near the ventilator and exhaust fans are 1376 ppm and 1123 ppm respectively. So the ventilator and exhaust fans play a major role to expel different obnoxious gases from the discussed kitchen. Site 4 can be considered as the nearest to an ideal kitchen by comparing different measured parameters with the ASHRAE standard.

2.2. Methods of measurement

For the experimental part of the present work, the concentration of CO₂, CO and temperature are recorded with the help of an indoor air quality measurement device - IAQ Calc7545 [15]. In each of the four kitchens, a 1.8 m × 1.4 m vertical area was selected, which is perpendicular to the vertical side of a burner that faces the cooks, and measurements were carried out at 72 suitable grid points within this area. The selected area is at the mid-plane of a burner, has a vertical extent of 1.8 m, and extends in the

horizontal direction such that the two sides lie respectively at 0.1 m and 1.5 m away from the burner. Measurements are also done in front of the burners on another vertical plane which is perpendicular to the previous measuring plane and is at 0.1 m away from the burner. A 1.8 m × 1.4 m area was selected, over which the measurements were carried out. The measurements were taken at 72 suitable grid points within this area.

Readings are taken with the help of IAQ Calc7545 in the constant key mode with a sampling interval of 5 s. The outside air conditions have also been recorded and are used as a basis of comparison for the conditions inside the kitchen. The Log Dat 2^M software [15] is used to export the stored data in the memory of the IAQ Calc recorder to an Excel spreadsheet for further processing. A velocity anemometer is used to measure velocities at various points on a cross-sectional plane in the vicinity of the exhaust fans; these data are used to determine the average flow rate through the fan.

2.3. Experimental results and discussion

The measured values of the concentration of CO₂ and CO, and of temperature are plotted in Figs. 2, 3 and 4 as a function of the distance from the gas burner. In order to avoid cluttering, for each of the three measured variables, values are shown here only at two different heights above the ground: of these, the height of 0.6 m indicates the position of the burner top and the height of 1.6 m is representative of the nose level or the typical breathing zone plane. The ASHRAE standards for different parameters of indoor air quality are given in Table 1, so that the measured data can be assessed in the proper context. The concentration level of different obnoxious gases and temperature of the four sites are discussed in the following sub-sections.

Now the concentration level of different obnoxious gases and temperature of four sites are considered separately.

2.3.1. Carbon-dioxide

Carbon-dioxide is a normal constituent of exhaled breath. The outdoor level of carbon-dioxide is usually 350–450 parts per million (ppm). The carbon-dioxide level is usually greater inside a building than outside. If the indoor carbon-dioxide level is more than 1000 ppm, when there is inadequate ventilation, there may be health implications and the occurrence of physical conditions such as headache, fatigue, and irritation of the eyes and the throat [16,17].

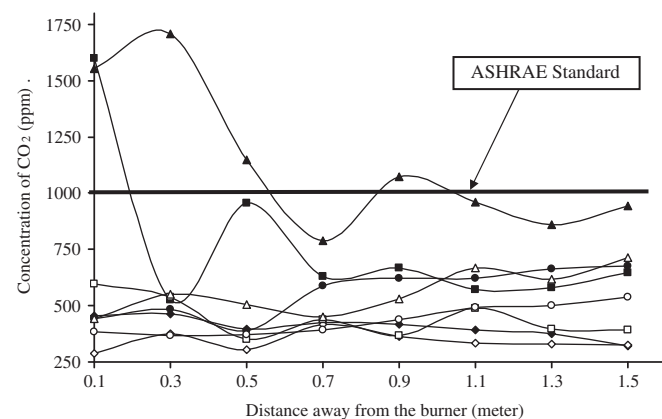


Fig. 2. Comparison of measured concentration of CO₂ at different heights as a function of the distance in various kitchens. Keys: —◆— experimental data of site 1 at height 1.6 m, —■— experimental data of site 2 at height 1.6 m, —▲— experimental data of site 3 at height 1.6 m, —●— experimental data of site 4 at height 1.6 m, —◇— experimental data of site 1 at height 0.6 m, —□— experimental data of site 2 at height 0.6 m, —△— experimental data of site 3 at height 0.6 m, —○— experimental data of site 4 at height 0.6 m.

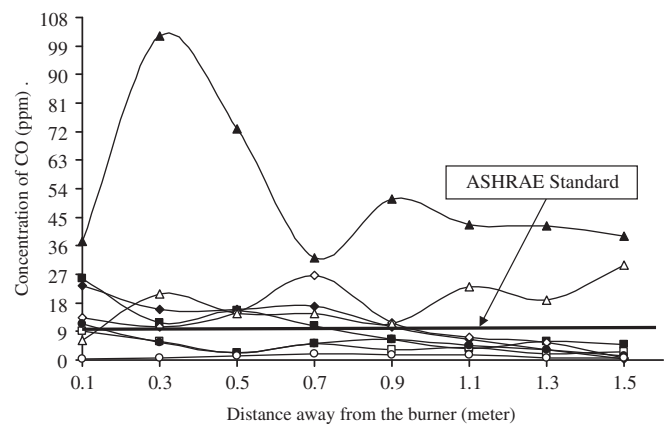


Fig. 3. Comparison of measured concentration of CO at different heights as a function of the distance in various kitchens. Keys: —◆— experimental data of site 1 at height 1.6 m, —■— experimental data of site 2 at height 1.6 m, —▲— experimental data of site 3 at height 1.6 m, —●— experimental data of site 4 at height 1.6 m, —◇— experimental data of site 1 at height 0.6 m, —□— experimental data of site 2 at height 0.6 m, —△— experimental data of site 3 at height 0.6 m, —○— experimental data of site 4 at height 0.6 m.

The measured values of CO₂ are shown in Fig. 2. The ASHRAE standard of CO₂ is also shown by a black bar in Fig. 2. The maximum concentration at nose level of site 1 is 462 ppm. It is observed at a distance 0.3 m away from the burner. So the level of concentration of CO₂ is well below the ASHRAE standard at site 1.

Site 2 is a kitchen with a natural exhaust hood. From the Fig. 2, it is seen that the concentration of CO₂ at nose level of site 2 decreases as one moves away from the burner. The maximum concentration of CO₂ is 1598 ppm at nose level at 0.1 m away from the burner. The level of CO₂ concentration is well above the ASHRAE standard up to a distance 0.2 m from the burner at nose level.

Site 3 is a kitchen which is small in size but serves food to a large number of customers. The pollutant and humid air are not exhausted to atmosphere due to the non-efficient architectural design. The level of CO₂ concentration in site 3 is well above the ASHRAE standard up to a distance 0.5 m away from the burner at nose level. The maximum concentration of CO₂ is 1710 ppm which is observed at a distance 0.3 m from the burner, which is the highest among the four kitchens studied. However, the measured

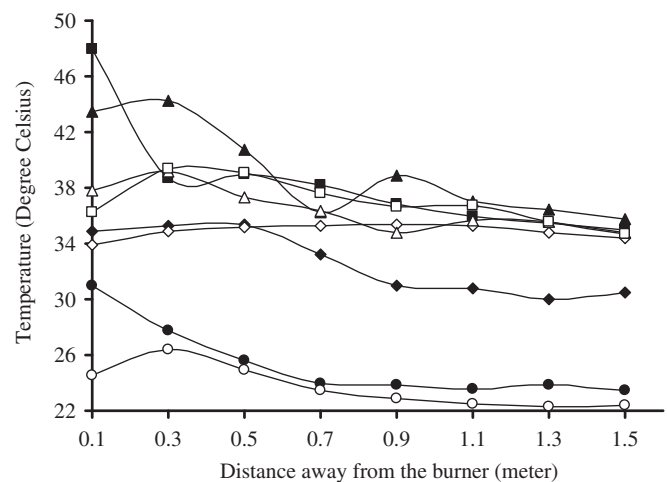


Fig. 4. Comparison of measured temperature (°C) at different heights as a function of the distance in various kitchens. Keys: —◆— experimental data of site 1 at height 1.6 m, —■— experimental data of site 2 at height 1.6 m, —▲— experimental data of site 3 at height 1.6 m, —●— experimental data of site 4 at height 1.6 m, —◇— experimental data of site 1 at height 0.6 m, —□— experimental data of site 2 at height 0.6 m, —△— experimental data of site 3 at height 0.6 m, —○— experimental data of site 4 at height 0.6 m.

Table 1
ASHRAE standard of different parameters.

S.L. no	Parameter	ASHRAE standard
1	Carbon-dioxide	1000 ppm
2	Carbon-monoxide	9 ppm
3	Temperature	20 °C to 26.1 °C

concentrations are well below the ASHRAE standard at the burner height. The above observations are found due to the convection phenomena as the hot obnoxious gases rise because of the buoyancy force. There are two exhaust fans in the kitchen. But they are unable to maintain healthy indoor air quality in the kitchen.

The maximum concentration of CO₂ at site 4 at nose level is 676 ppm. Fig. 2 shows that the concentration level of CO₂, both in site 1 and site 4, is well below the ASHRAE standard up to the nose level; however, the concentration is higher in site 4. In order to understand the interplay of the flow field and concentration distribution, the contour plot of CO₂ concentration in site 4 is shown in Fig. 5. The effect of the suction through the artificial hood exhaust system is clearly visible in Fig. 5. It has been described in Section 2.1 that there is very limited natural ventilation in site 4. Therefore, the combustion products are expelled from the site only through the hood exhaust system. This is why Fig. 5 shows that the concentration exceeds the ASHRAE standard near the hood inlet in site 4. For the same reason, a higher concentration of combustion products is present in site 4 as compared to site 1, and this trend persists even up to a large distance away from the burner, as shown in Fig. 2.

2.3.2. Carbon-monoxide

Carbon-monoxide is colourless and odourless, and is a normal constituent of exhaust gases from incomplete combustion. CO is dangerous (more so than CO₂) because it inhibits the blood's ability to carry oxygen to vital organs such as the heart and brain. For office areas, levels of carbon-monoxide are normally between 0 and 5 ppm [17]. Concentrations greater than 5 ppm indicates the possible presence of exhaust gases in the indoor environment and should be investigated. According to the ASHRAE standard, levels of carbon-monoxide inside buildings should not exceed 9 ppm (Table 1). An exposure to a CO level of 35 ppm may cause mild fatigue [17]. If the CO level inside a building is detected above 100 ppm, the building should be evacuated until the source is identified and the situation is corrected [17]. Adverse health effects such as headache and dizziness may occur after 2 h exposure to

carbon-monoxide concentrations of 100 ppm [17]. The above mentioned value for 8 h per day, five days per week.

The concentration of carbon-monoxide is high compared to the ASHRAE standard in all of the selected sites, as shown in Fig. 3. Site 1 is a spacious kitchen but it is not an ideal kitchen with respect to carbon-monoxide. The maximum concentration of CO is 23.5 ppm at a distance 0.1 m away from the burner which is shown in Fig. 3. The concentration of CO decreases as one moves away from the burner. The average concentration of CO at nose level is above 10.4 ppm up to a distance 0.9 m away from the burner. So nose level concentration of CO is well above the ASHRAE standard.

The maximum nose level concentration of CO in site 2 is 25.8 ppm at a distance 0.1 m away from the burner. The concentration of CO in site 2 is above ASHRAE standard up to a distance 0.7 m away from the burner. Fig. 6 depicts another interesting feature of site 2. The second burner from the left emits more amount of CO than the first one; this results in the observed asymmetry in pollutant concentration. So the operating condition of the burners is also an important factor in determining the indoor air quality.

Among the four kitchens studied, site 3 has the highest concentration of carbon-monoxide. The concentration of CO at nose level is well above 30 ppm at the farthest point from the burner, which is more than three times of the ASHRAE standard. The maximum concentration at nose level is 102.1 ppm at a distance 0.3 m away from the burner. All these features can be observed in Fig. 3.

In contrast to site 3, site 4 registers the lowest concentration level of CO at nose level among the four kitchens studied. The maximum measured value at nose level is 11.4 ppm. So the maximum concentration of CO at nose level is very near to the ASHRAE standard and the concentration is below the standard at most locations at nose level. This phenomenon is observed due to presence of artificial hood exhaust and well-conditioned burners.

2.3.3. Temperature

The measured distribution of temperature inside the four kitchens is shown in Fig. 4. The ASHRAE guideline is that indoor temperatures in the winter are maintained between 20 °C to 24 °C. Temperature in the summer should be maintained between 22.8 °C to 26.1 °C. Continuous exposure at high temperature may cause skin infections [17].

Measurements indicate that the temperature lies in the range of 30.5 °C to 35.4 °C in the site 1, as shown in Fig. 4. The maximum temperature is observed at the burner height. The outdoor

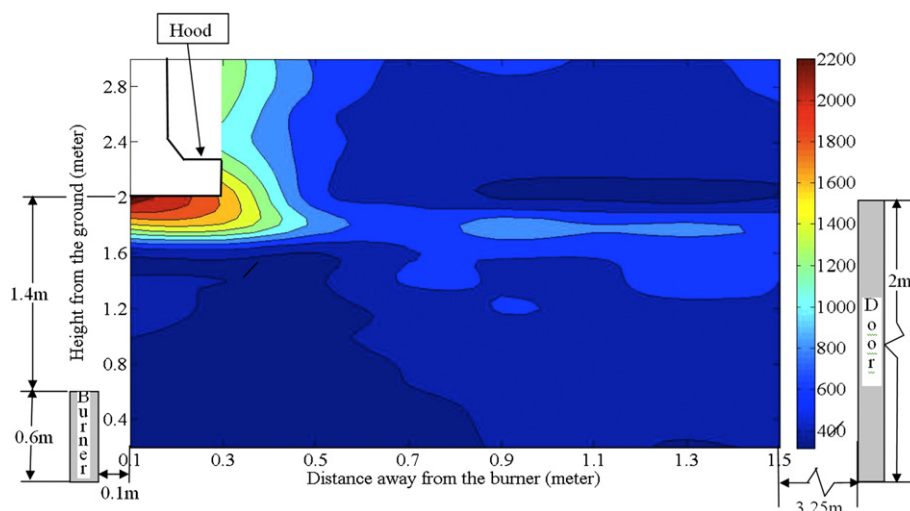


Fig. 5. Contour plot of CO₂ concentration (ppm) away from the burner in site 4.

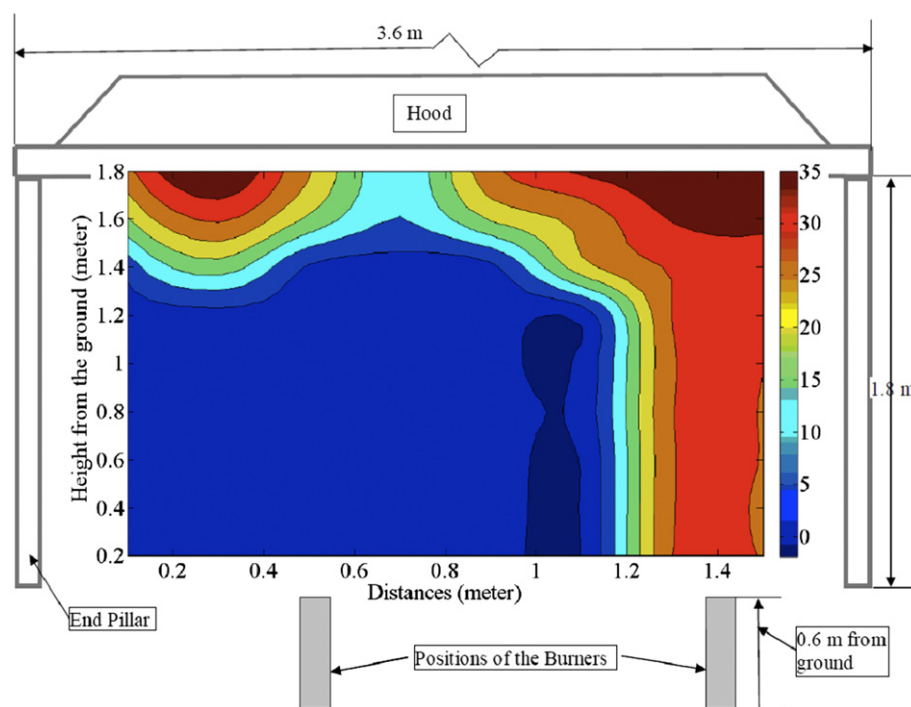


Fig. 6. Contour plot of CO concentration (ppm) at a plane 0.1 m away from the burners in site 2. The asymmetry in emission from the two burners shows the effects of burner characteristics on the indoor air quality.

temperature is 30 °C at the time of experiment, which is below the average room temperature. Hot air rises due to the buoyancy effect, but the exhaust fans are unable to extract the hot air completely. So the temperature of the room increases due to intermixing of the hot air and the colder air coming in the room through the open windows and doors. (So an air-conditioning unit will be required to maintain the temperature as per the ASHRAE standard.)

Among the four kitchens studied, the highest absolute temperature is measured in site 2. It is a very hot and humid kitchen. The temperature at 0.1 m away from the burner and 1.6 m from the ground is 48 °C, which is the maximum temperature in site 2 (this is in contrast to site 1, which does not have a hood system, where the maximum temperature occurs at the burner height). The outdoor temperature of site 2 is 31.4 °C. The hood is not able to capture hot gases completely. The hood is partially blocked due to dust, so an amount of back flow occurs.

Site 3 is also a hot and humid kitchen. The maximum temperature of site 3 is 43.5 °C, the outdoor temperature being 29.5 °C. During experimentation it is found that hot obnoxious gases blow towards the cooks (and the experimenters) due to an improper exhaust system. Air enters through a window and blows over the burner picking up the heat and combustion products, but there is no outlet at the opposite wall aggravating the situation. This is clearly visible in the contour plot of CO₂ distribution shown in Fig. 7; the contour plots of CO and temperature also demonstrate the same phenomena, but these figures are not included here.

It can be seen from Fig. 4 that the measured temperature in site 4 is lower, among all kitchens studied. The temperature in site 4 lies in the range 22.3 °C to 31 °C, the outdoor temperature being 22.5 °C at the time of the experiment. A summary of overall parameters for the four sites is given in Table 2. In order to be consistent with the data shown in Figs. 2, 3 and 4, the data in Table 2 also correspond to the two specific heights (0.6 m and 1.6 m, see Section 2.3).

From the above discussion it can be concluded that the indoor air quality of site 4 and site 1 is close to an acceptable standard, but this is achieved in two different ways. In site 4, a modern kitchen with

local exhaust ventilation (LEV) is responsible, whereas it is the general or dilution ventilation system and the large size of site 1 that achieve the desired effect. All measured parameters of site 2 and site 3 are well above the ASHRAE standards. So proper ventilation systems and air-conditioning units are required for these kitchens.

3. Numerical method and results

Computational fluid dynamics methods have been applied to determine the velocity field within the room of site 1 and to predict the distribution of pollutant concentration and temperature inside the room. The present study analyzes the characteristic of the flow field, velocity field and temperature field in the computational domain and tries to correlate all three fields to understand the indoor air quality of the computational domain.

3.1. Modelling description

The schematic model of site 1 is depicted in Fig. 8. This schematic model has been used for the numerical simulation. There are four windows and three doors and three exhaust fans in the model for ventilation purposes. The dimensions of the various important features of the kitchen are measured from the actual site and these values have been implemented in the numerical model. The length, width and the height of the model are 9.75 m, 6.09 m and 4.26 m respectively. The diameter of the exhaust fan is 0.46 m. The doors are 2.13 m long and 0.61 m wide. Each of the windows is 2.28 m long and 1.21 m wide.

3.2. Governing equations

The flow field in the domain has been computed by using three-dimensional, incompressible, steady Navier–Stokes equations with a two equation $k-\epsilon$ turbulence model. The temperature distribution in the computational domain is determined by simultaneously solving the energy equation.

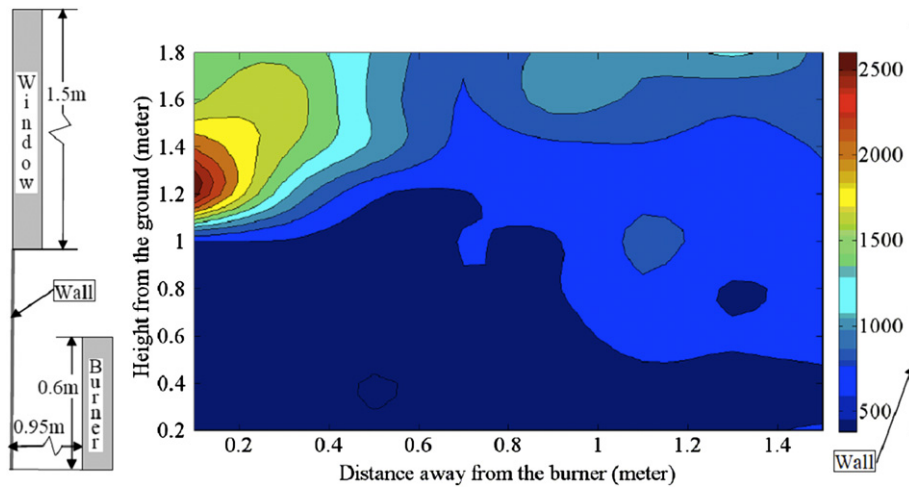


Fig. 7. Contour plot of CO₂ concentration (ppm) away from the burner in site 3.

The governing equations [18] are given below.
Continuity equation:

$$\frac{\partial \rho_m}{\partial t} + \nabla \cdot (\rho_m \vec{v}_m) = 0 \quad (1)$$

Momentum equation:

$$\frac{\partial}{\partial x_j} (\rho u_i u_j) = -\frac{\partial p}{\partial x_i} + \frac{\partial \tau_{ij}}{\partial x_i} + S_u \quad (2)$$

Energy equation:

$$\rho C_p \frac{DT}{Dt} = \nabla \cdot (K \nabla T) + \beta_1 T \frac{Dp}{Dt} + \lambda, \quad (3)$$

The $k-\epsilon$ model consists of the turbulent energy equation:

$$\frac{\partial}{\partial x_j} (\rho u_j k) = \frac{\partial}{\partial x_j} \left(\mu + \frac{\mu_t}{\sigma_k} \right) \frac{\partial k}{\partial x_j} + \mu_t G - \rho \epsilon, \quad (4)$$

And the dissipation rate equation:

$$\frac{\partial}{\partial x_j} (\rho u_j \epsilon) = \frac{\partial}{\partial x_j} \left(\mu + \frac{\mu_t}{\sigma_\epsilon} \right) \frac{\partial \epsilon}{\partial x_j} + \frac{\epsilon}{k} (C_1 \mu_t G - C_2 \rho \epsilon). \quad (5)$$

Volume fraction equation for secondary phases:

$$\frac{\partial}{\partial t} (\alpha_p \rho_p) + \nabla \cdot (\alpha_p \rho_p \vec{v}_m) = -\nabla \cdot (\alpha_p \rho_p \vec{v}_{dr,p}) \quad (6)$$

where,

$$\mu_t = C_\mu \frac{\rho k^2}{\epsilon} \quad (7)$$

$$\tau_{ij} = -(\mu + \mu_t) \left(\frac{\partial u_i}{\partial x_j} + \frac{\partial u_j}{\partial x_i} \right) \quad (8)$$

Table 2
Salient features of measured air quality.

Site no	Maximum CO ₂ concentration at nose level (ppm)	Maximum CO concentration at nose level (ppm)	Temperature range in the measuring plane (°C)	Maximum temp. in column 4 minus outdoor temp. (°C)
1	462	23.5	30–35.4	5.4
2	1598	25.8	34.7–48	16.6
3	1710	102.1	34.8–43.5	14.0
4	676	11.4	22.3–31	8.7

$$S_u = -\frac{2}{3} (\mu + \mu_t) \frac{\partial}{\partial x_i} \left(\frac{\partial u_i}{\partial x_i} \right) \quad (9)$$

$$\mu_t G = \mu_t \left(\frac{\partial u_i}{\partial x_j} + \frac{\partial u_j}{\partial x_i} \right) \frac{\partial u_i}{\partial x_j} - \frac{2}{3} \left(\rho k + \frac{\partial u_i}{\partial x_i} \right) \frac{\partial u_i}{\partial x_j} \quad (10)$$

The value of turbulent constants C_1 , C_2 , σ_k , σ_ϵ are 1.44, 1.92, 1 and 0.9 respectively [19].

3.3. Boundary conditions

The boundary conditions are listed below in Table 3. The room wall and the burner wall are solid and the no-slip boundary condition is applied there. The walls are also assumed to be impermeable. Pressure-inlet boundary condition has been imposed at the doors and windows. Fluent can automatically treat them as pressure-outlet boundaries if the velocity vectors point outward there. Zero gauge pressure is set at all pressure-inlet boundaries. There is a specific boundary condition called the ‘exhaust fan boundary condition’ available in Fluent, this is imposed on the two exhaust fans present in the computational domain. For this boundary condition, the pressure rise across the fan needs to be specified. This has been determined from the fan performance curve [20]. The fan performance curve gives a functional relation between the pressure rise and the flow rate. The flow rate has been determined experimentally in this work with the help of a velocity anemometer. The velocity was measured at several points over the cross-sectional area and from these the average flow rate of the exhaust fan is calculated as 587 L/s. The face of the burner is considered as velocity-inlet – the method of calculating the specified velocity is explained in Section 3.4.1. The turbulent intensity at the velocity-inlet has been set to 2% and the back flow turbulent intensity at all the pressure-inlet and exhaust fan boundaries have been set to 5%. The heat flux at the burner outlet, another boundary condition required by Fluent, is estimated by a simple thermodynamic calculation based on the known rate of fuel consumption. The specification of mole fractions of various species at the burner outlet, required as boundary conditions for Fluent, is discussed later in Section 3.4.1.

3.4. Details of the computational method

Computational fluid dynamics simulation of the flow of combustion products in the kitchen was performed using FLUENT 6.3.26 (2006) [18] software developed and marketed by Fluent, Inc.

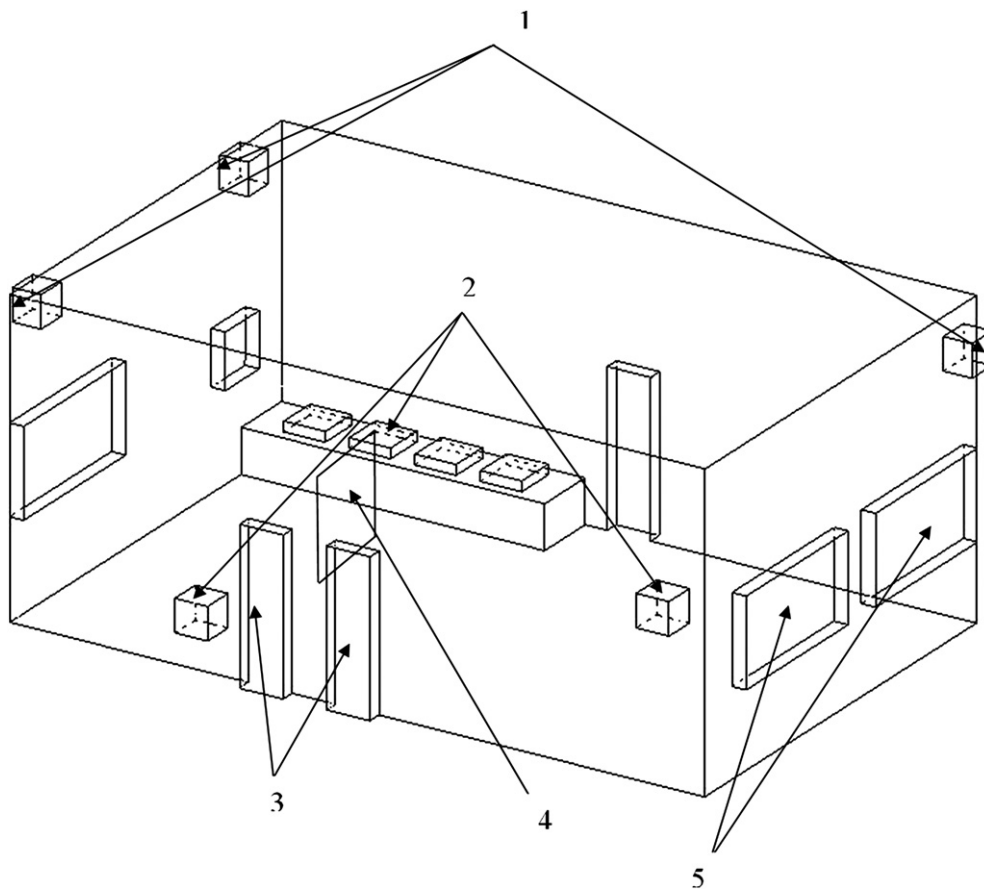


Fig. 8. Schematic diagram of computational domain of site 1. Keys: (1) exhaust fans, (2) burners, (3) doors, (4) experimental plane, (5) windows.

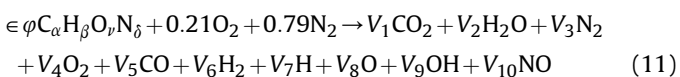
The model geometry and mesh were created using the GAMBIT 2.4.6 (2010) [21] software, also a product of Fluent, Inc. For this purpose a personal computer with a 2 GB RAM and 2.1 GHZ core 2 Duo processor was used. The goal of the simulation is to study the concentration of combustion products and the distribution of temperature at different parts of the kitchen. The computational procedure is validated by comparing the predictions with experimental results.

3.4.1. Mole fraction calculation

It is difficult to compute the complete combustion process at the burners with the help of Fluent. Therefore, the (approximately) correct temperature at the burners and the composition of the combustion products at the burner exit are calculated by a separate calculation process. The temperature and mole fractions of various chemical species, calculated by this separate method, are then used as input boundary conditions at the burner surface for the numerical simulation by Fluent. The CFD solution determines how these various chemical species released at the burner surface are then carried to various parts of the kitchen by the prevailing velocity field.

At first, mole fractions of combustion gases produced from combustion of propane gas, which is the major constituent of LPG, are obtained at a particular flame temperature and equivalence ratio by using a code [22] developed in FORTRAN. The code developed in FORTRAN is based on the combustion thermodynamics.

Combustion equation of any organic fuel can be written as



Atom balancing yields the following four equations

$$C \in \varphi \alpha = (y_1 + y_5)N \quad (12)$$

$$H \in \varphi \beta = (2y_2 + 2y_6 + y_7 + y_9)N \quad (13)$$

$$O \in \varphi \gamma + 0.42 = (2y_1 + 2y_2 + y_7 + y_9)N \quad (14)$$

$$N \in \varphi \delta + 1.58 = (2y_3 + y_{10})N \quad (15)$$

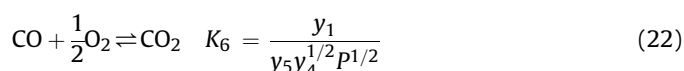
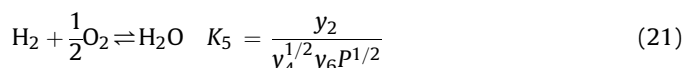
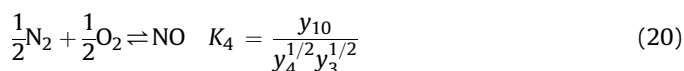
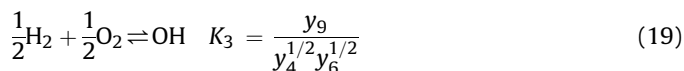
where $N = \sum_{i=1}^{10} V_i$ is the total number of moles. By definition, the following can be written

$$\sum_{i=1}^{10} y_i - 1 = 0 \quad (16)$$

Introduction of six equilibrium constants will yield eleven equations for the ten unknown mole fractions y_i and the number of moles. As reactions, consider the following

Table 3
Boundary conditions.

S.L. no	Part of the computational domain	Boundary conditions
1	Doors	Pressure-inlet
2	Windows	Pressure-inlet
3	Face of the burner	Velocity-inlet
4	Burner wall	Wall
5	Room wall	Wall
6	Exhaust fan	Exhaust fan



The value of the above equilibrium constants are found from Olikara and Borman relations.

Their expressions are of the form

$$\log K_p = \text{Aln}(T/1000) + \frac{B}{T} + C + DT + ET^2 \quad (23)$$

where T is in Kelvin. Olikara and Borman have curve-fitted the equilibrium constants to JANAF table [23] data. The values of A , B , C , D , E are different for different equilibrium constants. In our case, the fuel is propane: hence we set $\alpha = 3$, $\beta = 8$, $\gamma = 0$, $\delta = 0$.

The (approximately) correct temperature and the equivalence ratio were determined by a painstaking, iterative process. The process started with a good educated guess about the values of the two parameters. Then the FORTRAN code was run, which gave the mole fractions of various combustion products. The flow field of the kitchen was then determined by running Fluent, with the mole fractions as the input at the boundaries representing the burner surface. The computationally determined concentration of CO_2 at the nose level of the cook was then compared with the measured value. If the difference between the computational and experimental values was larger than a set tolerance, then the calculation process is repeated by an improved guess of the temperature and equivalence ratio.

After a number of iterations, it was found that a temperature of 1240 K and an equivalence ratio of 1.03 would give the best match. After running the FORTRAN code [22] for this condition, the results obtained are the mole fractions of different combustion products produced from combustion of propane gas per 1 mol air consumed; these calculated values are given in Table 4 and are used as the boundary conditions for the Fluent simulations. From the mole fractions and fuel consumption rate, volume fraction of combustion gases and velocity of combustion mixture are obtained, which are used in the multiphase flow modelling module of the Fluent software.

3.4.2. Creation of geometry and mesh using Gambit 2.4.6

The geometry of the kitchen was first created by creating a box with the dimensions of the kitchen. The doors, windows, exhaust fans were then created as extended volumes and were then united with the original volume. The burners were created using the method of subtraction. Initially the volumes were uniformly meshed with HEX – sub map mesh with interval size of 0.2 m. Number of mesh cells generated were 31869 cells. The grid independency test is described later in Section 3.6.

3.4.3. Application details for FLUENT

After importing mesh file to FLUENT, the grid was checked. Then energy model and multiphase – mixture model were opted and

Table 4
Mole fraction calculation.

S.L. no	Combustion products	Mole fractions
1	CO_2	0.0689
2	H_2O	0.0935
3	N_2	0.8229
4	CO	0.00608
5	H_2	0.00545

number of phases were taken as 7. Standard $k-\epsilon$ model was chosen for turbulence modelling. The various combustion products, viz. carbon-dioxide, carbon-monoxide, hydrogen, nitrogen and water vapour, were chosen as different phases. In the Fluent menu 'operating conditions', gravity is selected and is set to $-9.81 \text{ m}^2/\text{s}$.

The mixture model is designed for two or more phases (fluid or particulate). Phases are treated as interpenetrating continua. The mixture model solves the mixture momentum, continuity, energy equations and prescribes the relative velocities to describe the dispersed phases assuming local equilibrium over short spatial length scales.

The accuracy of using computational fluid dynamics as a tool for the prediction of flow features depend on the choice of the turbulence model. The standard $k-\epsilon$ model is the most common turbulence model and it is routinely used for indoor environment analysis [24]. It also provides the easiest convergence in its formulation. The model-dependent constants are determined empirically from a number of case studies [19]. In the RNG $k-\epsilon$ model, on the other hand, almost all of the coefficients are deduced theoretically. After comparing five $k-\epsilon$ models, reference [24] recommended the RNG model as being the most appropriate for simulating indoor air flow patterns. Apart from the RNG model, ref [24] noted that the standard $k-\epsilon$ model is also suitable for indoor air flow analysis. In the present case, due to the complexity of the geometry, the Standard $k-\epsilon$ model is chosen for the easiest convergence.

Fluent is based on Finite volume method (FVM) to solve the continuity, momentum and energy conservation equations. In the present study the above equations were solved in pressure based solver. SIMPLE algorithm has been used for pressure–velocity coupling for the pressure correction equation. First order upwind scheme (for convective variables) was considered for momentum as well as for turbulent discretized equations. For all simulations the solution was considered to be steady state. In all simulations the solution was considered to be converged if the scaled residuals reached 10^{-4} for momentum and continuity and 10^{-7} for the energy equation. Under-relaxation factors of 0.3 for pressure, 0.7 for momentum, 0.5 for k and ϵ , and 1 for energy were used for the convergence of all the variables.

3.5. CFD results and discussion

The numerical solutions of the flow field, and the distribution of temperature and concentration of chemical species in site 1 are analyzed in this Section.

3.5.1. Velocity field

Fig. 9 represents snapshots of velocity vectors in different planes showing the circulation of air and combustion products in different parts of the room. The colour of the arrow gives the magnitude of velocity and the direction of the arrow gives the direction of the flow. While specifying the boundary conditions, all windows and doors were considered as pressure-inlet whereas the exhaust fan was considered as exhaust fan boundary conditions (Section 3.3). But the converged solution shows an interesting phenomenon. One

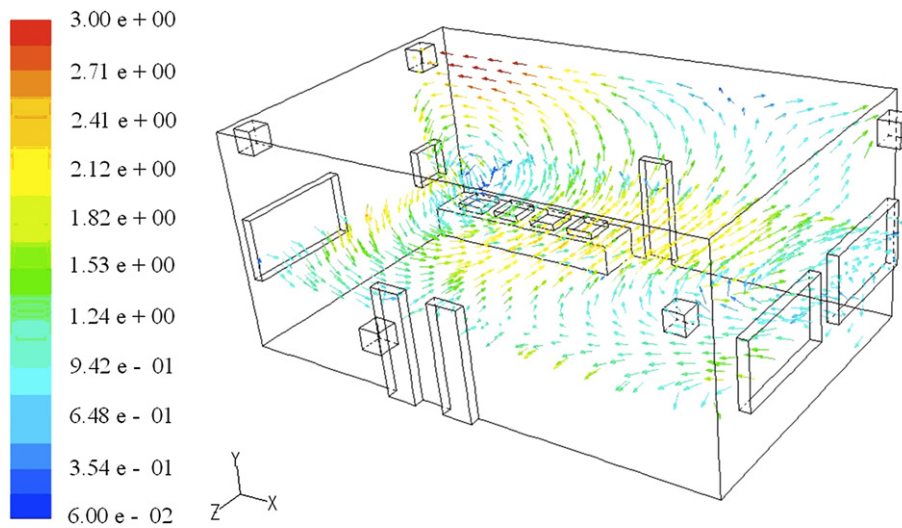


Fig. 9. Computed 3-dimensional velocity vectors on two intersecting planes of site 1 in Fluent. (Colours denote magnitude of velocity in m/s). (For interpretation of the references to colour in this figure legend, the reader is referred to the web version of this article.)

can see from the plotted velocity vectors in Fig. 5 that air enters in the kitchen through all doors and windows except the window at the right corner. Air exits through the right corner window. This shows that specifying the boundary conditions at all windows and doors as “pressure-inlet” in Fluent did not predetermine the direction of flow through these openings. The converged solution evolves such that the correct direction of velocity vectors is automatically achieved. A circulation is produced near the cooking area due to the high temperature of combustion gases. Air is exhausted through the exhaust fan.

3.5.2. CO₂ concentration distribution

For a better understanding of the flow pattern and concentrations of various combustion gases, we have considered contours and velocity vectors in two mutually perpendicular planes at 1.6 m height and 0.1 m away from the burner. For showing the concentration of CO₂, the horizontal plane is chosen at the nose level (Fig. 10), since the inhalation of this gas is harmful for the cooks. The vertical plane is chosen at 0.1 m away from the burner as this represents the normal

positions of the cooks when they are cooking. From Fig. 10, one can see that the computed concentration near the burner is above 450 ppm. The concentration of CO₂ increases due to improper exhaust condition. Near the doors and windows, lower concentrations of around 300 ppm can be seen due to proper air flow from the outside. In the rest of the room the concentration varies around 400 ppm which is well within the acceptable limits. So site 1 is near to an ideal kitchen with respect to CO₂ concentration. The computational result agrees with the experimental result (Fig. 2).

3.5.3. CO concentration distribution

Like CO₂, the computed CO concentration is also shown on two mutually perpendicular planes; the reasons for selecting these planes are the same as explained in Section 3.5.2. From Fig. 11, one can see that the computed average concentration near the burner rises up to 19.5 ppm which is well above the ASHRAE standard. From the experimental data (Fig. 5) it can be seen that the concentration of CO is above 18 ppm up to 0.3 m away from the burner. So the experimental data validates the computational result. It is also

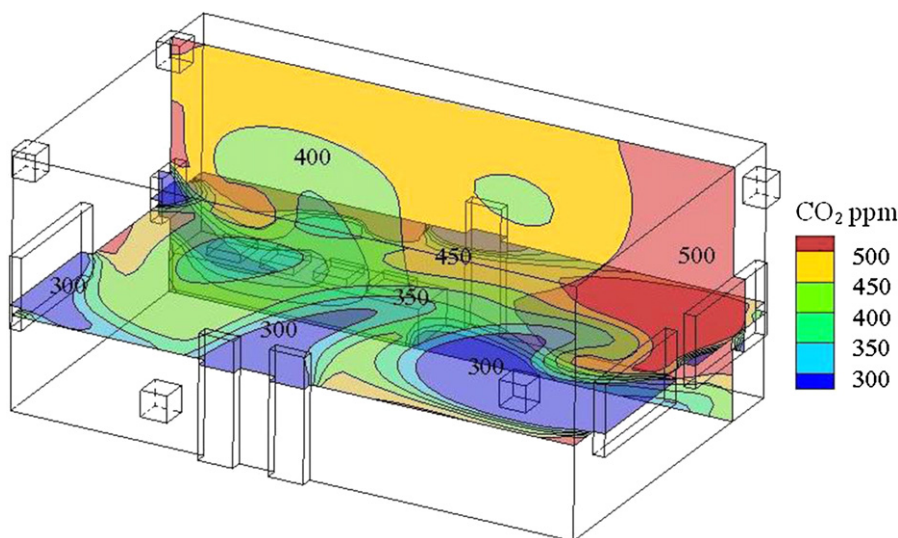


Fig. 10. CO₂ concentration distribution, computed by Fluent, on two intersecting planes of site 1.

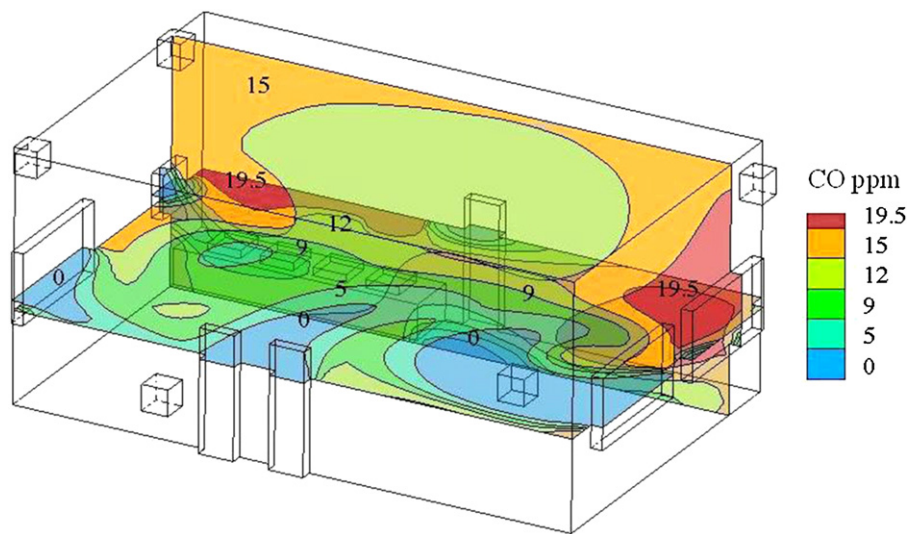


Fig. 11. CO concentration distribution, computed by Fluent, on two intersecting planes of site 1.

depicted in Fig. 11, that as one moves away from the burner, the level of CO decreases drastically and drops to a negligible value.

3.5.4. Temperature distribution

The computed temperature field at 0.6 m above the ground is depicted in Fig. 12. The temperature distribution is also shown on two intersecting planes: the vertical one is 0.1 m away from the burners (like the case of CO₂ and CO) but the horizontal plane is 0.6 m above the ground (i.e. at the height of the top of the burner). The temperature is quite high near the burner, around 36 °C, while near the window it is 32 °C. From the experimental data (Fig. 7), one finds that temperature near the burner is 35.2 °C at 0.5 m away from the burner. So the experimental data validates the temperature distribution in the computational domain. From Fig. 12, one can see that the temperature decreases and returns to outdoor temperature as one moves away from the burner.

3.6. Grid independency

The test for grid independency is an essential part of a dependable CFD simulation. Grid independency is also known as the

consistency of discretized solutions. One has to make sure that the numerical solution is not significantly dependent on the size of the grids adopted. In other words, the chosen size of the grids should be adequate for resolving the relevant thermo-fluid dynamic scales. The grid independency is also a check for conservation and boundedness of the solution. To demonstrate the accuracy of the presented numerical results, a systematic grid independency test has been carried out, in addition to validating the results by conducting experiments (described in Section 3.7).

Grid independency was established by progressively refining the mesh size by the ‘region adaptation method’ and comparing the various results. At first for CFD simulation the room domain was discretized to 31869 cells of 0.2 m Hex element. ‘Submap’ scheme was used to discretize the domain. When the computational domain was simulated with a finer mesh of Hex 40218 cells, the difference between the average concentrations of CO₂, CO and temperature distribution in the breathing zone plane (1.6 m height from the ground) were found to be 5%, 5.2%, 6% respectively. So again the simulation was performed with Hex 63468 cells. Now the difference between the average concentrations of CO₂, CO and temperature distribution in the breathing zone plane were found to

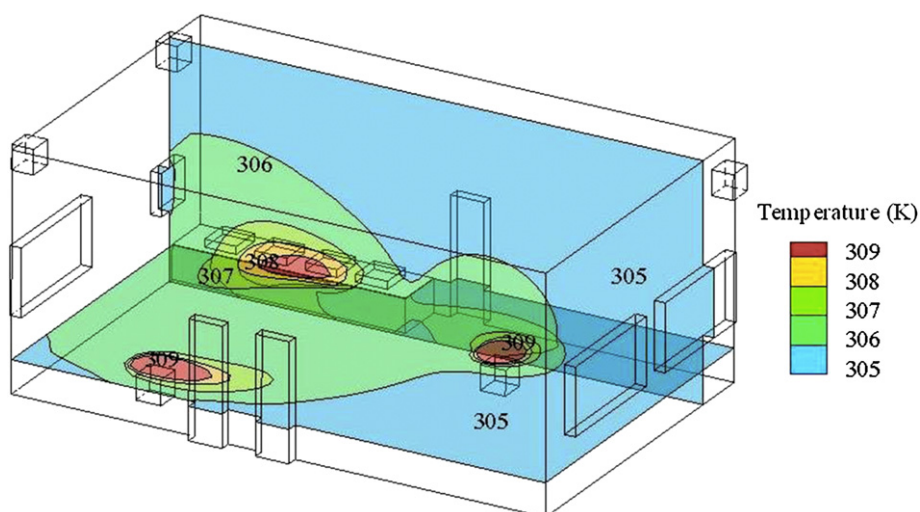


Fig. 12. Temperature distribution, computed by Fluent, on two intersecting planes of site 1.

Table 5
Comparison between experimental values with simulation results.

S.L. no	Parameter	Experimental values	Simulation results
1	Carbon-dioxide (ppm)	455–425	485–442
2	Carbon-monoxide (ppm)	23.5–15.8	19.2–15
3	Temperature (°C)	35.4–34.9	34.1–33.7

be 0.1%, 0.85%, 1.55% respectively. It was decided that the grid independence is achieved for the present purpose, and the grid with Hex 63468 cells has therefore been adopted for numerical simulations.

3.7. Comparison with full scale experiment

Finally, to further validate the accuracy of the numerical simulations undertaken, the predicted temperature field and the distribution of chemical species are compared with the experimental values measured in the present work. A comparison of the simulated and measured CO₂, CO concentrations and temperature from distance 0.1 m to 0.5 m away from the burner in the breathing zone plane (1.6 m from the ground) are presented in Table 5. Distance 0.1 m to 0.5 m away from the burner is considered here because this represents the main cooking area which is our region of interest. For CO₂ and CO concentration and temperature distribution fairly good agreement was found, though the experiment gave slightly higher concentrations and temperature.

This difference may have been caused by the measurement errors, e.g. the data were not taken at a true steady state. Basically there is no real steady state for such a kitchen because the ambient conditions were continuously changing while in the simulation the averaged ambient conditions were used. The flow rate through the burner is also varied in the experimental condition (as the cooks adjusted the burners depending on the various stages of a cooking process). The experimental data also changes with the time-dependent use of various kitchen appliances. (For example, it is found that the species concentrations changed as the cooks moved the ladle to stir the cooking materials in large pans). The effects of metabolism and activities of the workers of the kitchen are also not incorporated in the computational modelling. The discrepancies found here between CFD simulation and experimental observation may also have resulted from insufficiently detailed representation of other boundary conditions. It may be possible to further improve CFD results by using a more refined representation of other boundary conditions, such as wall temperature, velocity profile at doors and windows. In addition more sophisticated treatment of turbulence, wall effects and finer grid near the burner may also improve CFD performances.

4. Theoretical studies of one improved design of the site 1

In this section we propose one modification of the existing design to improve the indoor air quality of the selected kitchen. Only architectural design improvement is incorporated in the modified design, to be designated in the following discussion as

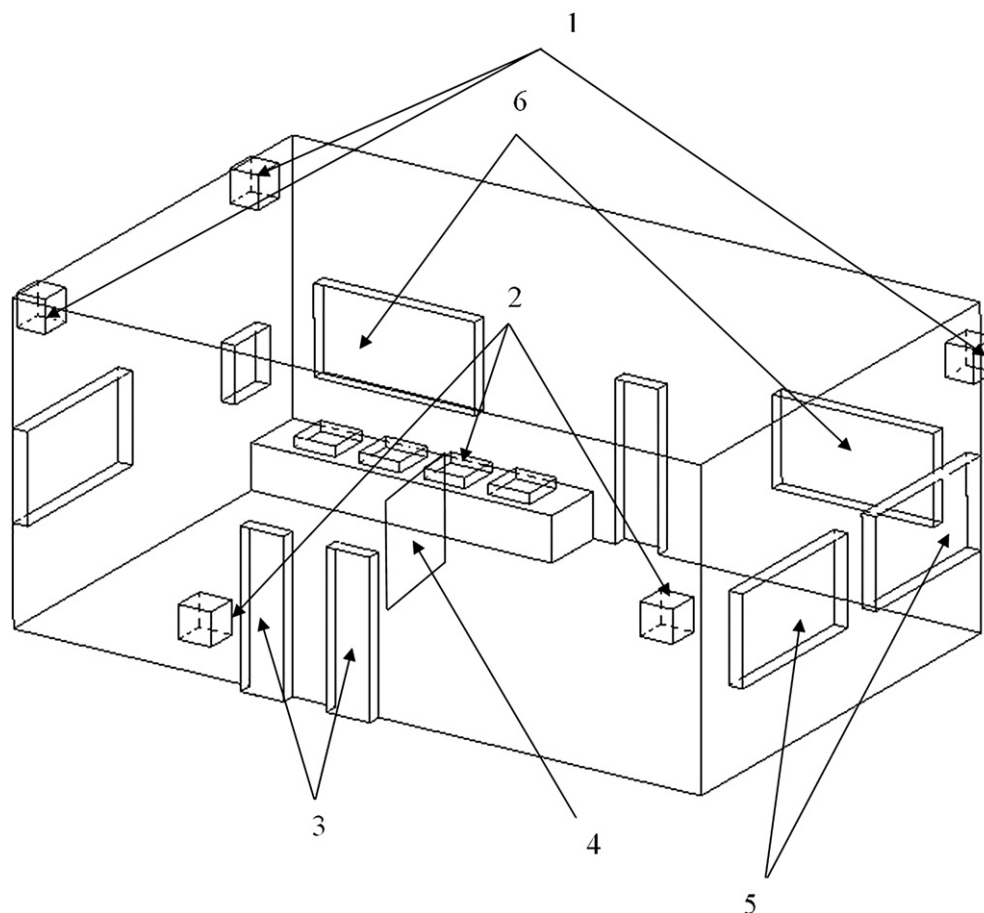


Fig. 13. Schematic diagram of computational domain of the improved design named Revision-1. Keys: (1) exhaust fans, (2) burners, (3) doors, (4) experimental plane, (5) windows, (6) proposed windows.

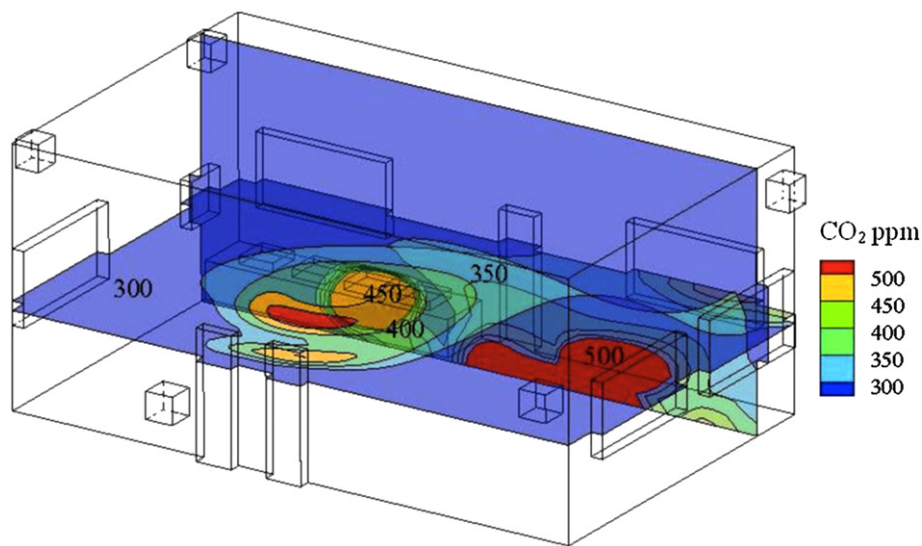


Fig. 14. Computed CO₂ concentration distribution on two intersecting planes: computations carried out with Fluent for the improved design Revision-1.

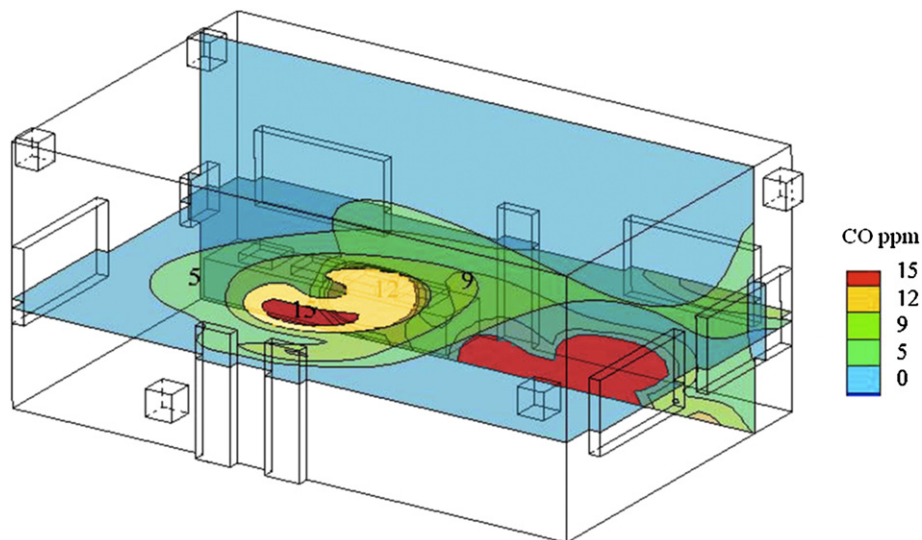


Fig. 15. Computed CO concentration distribution on two intersecting planes: computations carried out with Fluent for the improved design Revision-1.

Revision-1. Two new windows are added to the existing design, the locations and sizes of the new windows being chosen on the basis of educated guess to improve the air circulation in the room. The schematic diagram of the modified design is shown in Fig. 13 which may be compared with Fig. 8. The same software Fluent is used for the CFD simulations for Revision-1 in the same manner described in Section 3. The main findings from these computations are summarized in Figs. 14 and 15.

Fig. 14 shows that the accumulation of CO₂ is greatly reduced due to the architectural design improvement, although some accumulation of CO₂ can still be seen near the burners in Fig. 14. The concentration of CO₂ lies between 300 ppm and 500 ppm in the improved design. Fig. 15 shows that the concentration of CO is drastically reduced by incorporating two windows in the revised design, though the concentration is still above the ASHRAE standard in some portions of the computational domain.

This simple computational exercise shows that judicious architectural design, with the focus on the indoor air quality, may achieve much improved working environment without the requirement of extra investment. This may be important in the

context of developing countries where investments for installing specific appliances may not always be possible.

5. Conclusion

This study investigated and analyzed the three-dimensional flow field and the distribution of temperature, CO₂ and CO in four large kitchens. The four kitchens have been carefully selected to represent a variety of architectural designs, physical arrangements of the cooking apparatus and exhaust systems. The investigation is performed both experimentally and numerically. How the distributions of CO₂, CO and temperature are related with the architectural design, physical arrangement and fluid flow field has been explored. The desirable and undesirable features and elements in the design of a large community kitchen can be appreciated from the experimental and computational results for the four kitchens presented here.

It is hoped that the study would establish a focus on and an improvement in the indoor air quality in the future designs of large kitchens, particularly in developing countries where adequate fund

for installing specific appliances may not always be available. A computational study summarized in Section 4 shows possible great improvement in indoor air quality for relatively modest alteration in the architectural design. The present experimental study described in Section 2 shows that the indoor air quality of site 4 and site 1 is close to an acceptable standard, but this is achieved in two different ways. In site 4, local exhaust ventilation (LEV) systems for each burner are responsible, whereas it is the general or dilution ventilation system and the large size of site 1 that achieve the desired effect.

The experiments for the present study were carried out in situ during normal operational hours without disrupting the activities of the cooks and support staff. This makes the experimental data particularly useful for designing and assessing similar kitchens. The experimental results also reveal several subtle flow physics. For example, Fig. 5 shows the build-up of obnoxious gases near the suction hood (a cook's normal position of the nose should therefore be away from this zone), the disparity in the emissions from the two burners shown in Fig. 6 inform us about the importance of the burner condition in maintaining indoor air quality, Fig. 7 reveals how an improperly designed ventilation system may blow hot obnoxious gases towards the cooks.

A computational procedure for determining the three-dimensional distribution of temperature and hazardous gases (such as CO₂ and CO) inside an operational kitchen has been formulated in the present study. The task is difficult because of complex three-dimensional features of the computational geometry and complex sets of boundary conditions. A computational method has been developed here for determining the volume fractions of CO₂ and CO at the outlet of the burners that can be used as the input boundary conditions of the CFD flow solver (such as Fluent). The CFD simulations performed in the present work agree well with the experimental results for the selected site 1. This direct validation by comparing with present experimental results obtained in the same site gives confidence in the computational procedure devised here.

References

- [1] Thiebaut HP, Knize MG, Kuzmicky PA, Hsieh DP, Felton JS. Airborne mutagens produced by frying beef, pork and a soy-based food. *Food Chem Toxicol* 1995; 33(10):821–8.
- [2] Vainiotalo S, Matveinen K. Cooking fumes as a hygienic problem in the food and catering industries. *Am Ind Hyg Assoc J* 1993;54(7):376–82.
- [3] Guha A. A unified Eulerian theory of turbulent deposition to smooth and rough surfaces. *J Aerosol Sci* 1997;28(8):1517–37.
- [4] Guha A. Transport and deposition of particles in turbulent and laminar flow. *Ann Rev Fluid Mech* 2008;40(1):311–41.
- [5] Ng TP, Hui KP, Tan WC. Respiratory symptoms and lung function effects of domestic exposure to tobacco smoke and cooking by gas in non-smoking Women in Singapore. *J Epidemiol Community Health* 1993; 47(6):454–8.
- [6] Li Y, Delsante A. Derivation of capture efficiency of kitchen range hoods in a confined space. *Build Environ* 1996;31(5):461–8.
- [7] Khan JA, Feigley CE, Lee E, Ahmed MR, Tamanna S. Effects of inlet and exhaust locations and emitted gas density on indoor air contaminant concentrations. *Build Environ* 2006;41(1):851–63.
- [8] Chung KC, Hsu SP. Effect of ventilation pattern on room air and contaminant distribution. *Build Environ* 2001;36(1):989–98.
- [9] Srebić J, Vukorvić V, He G, Yang X. CFD boundary conditions for contaminant dispersion, heat transfer and air flow simulations around human occupants in Indoor environments. *Build Environ* 2008;43(1):294–303.
- [10] Chiang CM, Lai CM, Chou PC, Li YY. The influence of an architectural design alternative (transoms) on indoor air environment in conventional kitchens in Taiwan. *Build Environ* 2000;35(1):579–85.
- [11] Reggio M, Abanto J. Numerical investigation of the flow in a kitchen hood system. *Build Environ* 2006;41(1):288–96.
- [12] Lee E, Feigley C, Khan J. An investigation of air inlet velocity in simulating the dispersion of indoor contaminants via computational fluid dynamics. *Ann Occup Hyg* 2002;46(8):701–12.
- [13] Atlanta GA. ASHRAE STANDARD 62-1982: ventilation for acceptable air quality. American Society of Heating, Refrigerating and Air Conditioning Engineers, Inc.; 1989.
- [14] Burgess WA, Ellenbecker MJ, Treitman RD. Ventilation for control of the work environment. 2nd ed. New York: John Wiley & Sons; 2004.
- [15] Manual for IAQ-CALC indoor air quality meter. 500 Cardigan Road, Shore View, M.W 55126, USA: TSI Incorporated; August 2008.
- [16] Aerias, Air Quality Sciences, IAQ resource centre.
- [17] Quinn P, Arnold DT. Environmental health fact sheet. Springfield, Illinois 62701: Illinois Department of Public Health; 2010.
- [18] Fluent 6.3.26, user guide. Fluent Inc; 2006.
- [19] Lee C, Lim K. A numerical study on the characteristics of flow field, temperature and concentration distribution according to changing the shape of separation plate of kitchen hood system. *Energy Build* 2008;40(1):175–84.
- [20] Daly BB. Woods practical guide to fan engineering. 3rd ed. Colchester: Woods of Colchester Limited; 1978.
- [21] Gambit 2.4.6, user guide. Fluent Inc; 2010.
- [22] Ferguson CR. Internal combustion engines. 1st ed. New York: John Wiley & Sons; 1986.
- [23] Chase MW, Curnutt JL, Hu AT, Prophet H, Syverud AN, Walker LC. JANAF thermochemical tables, 1974 Supplement. Thermal Research, The Dow chemical company, Midland, Michigan 48640.
- [24] Chen Q. Comparison of different $k-\epsilon$ models for indoor air flow computations. *Numer Heat Transfer* 1995;28(B):353–69.

Nomenclature

- c_p : Specific heat at constant pressure
 K : Thermal Conductivity
 k : Turbulent kinetic energy
 N : Total number of moles
 P : Pressure
 S_u : Source term
 T : Temperature
 $\vec{v}_{dr,p}$: Drift velocity for secondary phase p
 V_i : Number of moles
 \vec{v}_m : Mass averaged velocity
 y_i : Mole fraction
 α_p : Volume fraction of secondary phase
 β_i : Thermal expansion coefficient
 ϕ : Equivalence ratio
 λ : Source term in energy equation
 μ : Dynamic viscosity
 μ_t : Turbulent viscosity
 ρ : Density
 ρ_m : Mixture density
 τ_{ij} : Shear stress
 ϵ : Dissipation energy
 ϵ : The molar fuel-air ratio
- Subscripts**
 α : Number of Carbon atoms
 β : Number of Hydrogen atoms
 γ : Number of Oxygen atoms
 δ : Number of Nitrogen atoms
 i : Phase number (Eq. (16))
 p : Secondary phase (Eq. (6))